


Cite this: *Chem. Sci.*, 2025, 16, 19414 All publication charges for this article have been paid for by the Royal Society of ChemistryReceived 28th May 2025
Accepted 12th September 2025

DOI: 10.1039/d5sc03892h

rsc.li/chemical-science

Sequential one-pot *N*-alkylation and aminocarbonylation of primary amines catalyzed by heterobimetallic Ir/Pd complexes

Amin Abdollahi, Philipp Woite, Konrad Kretschmar, Michael Roemelt, *
Thomas Braun * and Ouchan He

The paper introduces bimetallic Ir/Pd complexes as catalysts to initiate an *N*-methylation coupled with an aminocarbonylation in a one-pot approach, in order to advance the field of carboxamide synthesis. The iridium center initiates the reaction by selectively facilitating the *N*-methylation through amination, while the palladium center, in a complementary role, drives the carbonylation step. This bimetallic synergy not only streamlines the reaction sequence but also surpasses the efficiency and selectivity of monometallic Ir or Pd catalysts. Mechanistic studies suggest the presence of catalytically active hydride species within the *N*-methylation cycle, which were characterized experimentally and *via* quantum chemical calculations. The developed synthetic routes offer a sustainable, cost-effective, scalable and also unprecedented preparation method, with the bimetallic catalysts being robust and versatile.

Introduction

Sequential one-pot catalysis involves multiple catalytic steps in a set sequence, allowing intermediates from one step to serve as substrates for the next without isolation or purification. This method enhances efficiency in organic synthesis by linking different reactions in one-pot, reducing solvents, catalysts, workup procedures, and reaction times.^{1–4} However, catalysts must be compatible with both reaction steps with respect to reaction conditions and lifetimes.^{1–9}

Bimetallic catalysts, particularly heterobimetallic ones, are promising for sequential catalysis, where two different metal centers synergistically catalyze multiple reaction steps. This can lead to improved or unique reactivities and selectivities compared to homobimetallic or monometallic catalysts.^{10–32} While processes enhancing the activity of heterobimetallic complexes compared to their monometallic counterparts are well-established, the one-pot activity for sequential reaction pathways remains limited.^{33–38} An array of late–late bimetallic transition metal complexes has been synthesized to serve as unique catalysts in diverse C–N/C–C bond coupling reactions.^{39–43} Notably, bimetallic Pd(i) and Pd(ii) complexes exhibit activity in aminocarbonylation of primary amines and Buchwald–Hartwig aminations.⁴⁴ A heterobimetallic catalyst featuring Ir/Pd centers and a 1,2,4-trimethyltriazolyldiylidene ligand (ditz) was employed to catalyze tandem imine formation from corresponding nitroarenes.⁴⁵ Furthermore, three sets of Ir/Pd complexes with the mentioned bridging ligand were

synthesized and utilized in tandem reactions involving various transformations of halo-acetophenones. These transformations encompass (i) dehalogenation and transfer hydrogenation, (ii) Suzuki coupling and transfer hydrogenation, and (iii) Suzuki coupling and α -alkylation with primary alcohols.⁴⁶

In this paper we report on the synthesis of Ir/Pd bimetallic complexes and their application in a one-pot process for mono-*N*-methylations of primary amines under air, coupled with aminocarbonylations of the resulting secondary amine under atmospheric CO pressure. Model studies gave mechanistic insights by identifying catalytically relevant hydride species, which were also characterized by means of quantum chemical calculations (Fig. 1).

Routes to bimetallic Ir/Pd complexes bearing imidazole or pyridine based bridging phosphine ligands were developed. The bimetallic compounds [IrPd(Cl)₃(CO)(PiPr₂Im)₂] (Im = imidazole) (**4**), [IrPd(Cl)₃(CO)(PiPr₂Im^{Me})₂] (Im^{Me} = 1-methyl-1*H*-imidazole) (**5**) and [IrPd(Cl)₃(CO)(PPh₂Py)₂] (Py = pyridine) (**6**) were synthesized by treatment of the corresponding mononuclear Ir complexes *trans*-[Ir(Cl)(CO)(PiPr₂Im)₂] (**1**), *trans*-[Ir(Cl)(CO)(PiPr₂Im^{Me})₂] (**2**) and *trans*-[Ir(Cl)(CO)(PPh₂Py)₂] (**3**) with [Pd(Cl)₂(COD)] (Scheme 1). The complexes **3** and **6** (Scheme 1) have been reported before, but **6** was synthesized *via* an alternative route.⁴⁷ Other binuclear complexes featuring 2-(diphenylphosphino)pyridine (Ph₂PPy) as a bridging ligand with iridium centers have also been described.^{49–51} The bimetallic Ir/Pd complexes were characterized by ¹H NMR, ³¹P{¹H} NMR, and IR spectroscopy (see SI). Notably, the IR spectrum of **4** displays a very broad absorption band at $\tilde{\nu} = 3091\text{ cm}^{-1}$ for the NH unit, which is shifted to lower frequencies compared to the NH absorption frequency of **1** at 3343 cm^{-1} . The NMR and IR data

Department of Chemistry, Humboldt-Universität zu Berlin, Brook-Taylor Str. 2, 12489 Berlin, Germany. E-mail: thomas.braun@cms.hu-berlin.de



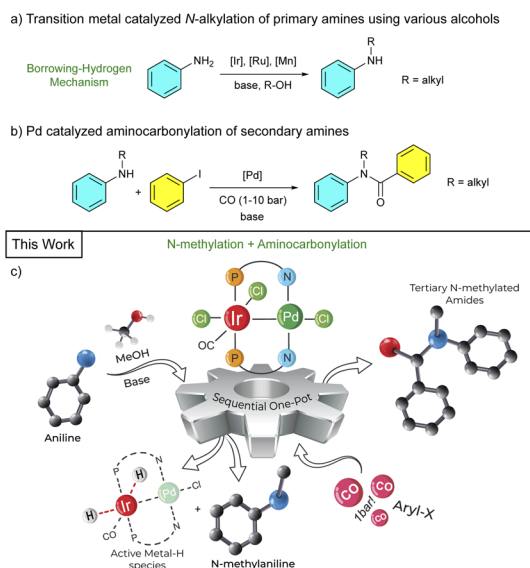
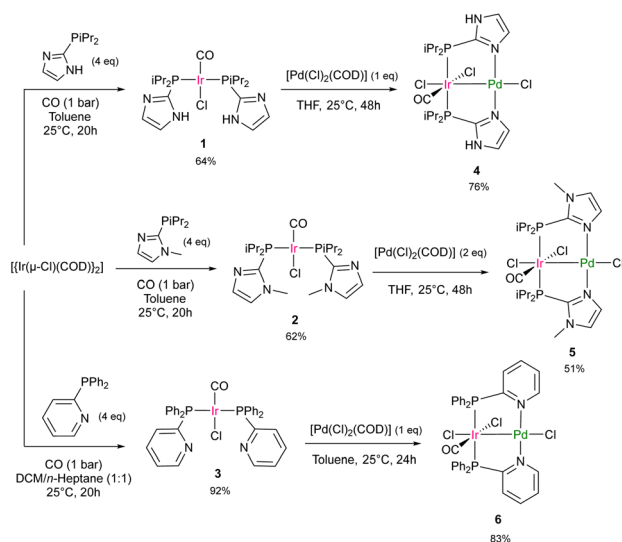


Fig. 1 (a) Transition metal-catalyzed *N*-alkylation. (b) Pd-catalyzed aminocarbonylation. (c) Sequential one-pot *N*-alkylation followed by aminocarbonylation of primary amines.



Scheme 1 Routes to the complexes 4, 5, 3 and 6.⁴⁷

suggest the presence of hydrogen bonding.^{52,53} Strong absorption bands for the terminal-bound CO were detected between 1950 and 2016 cm^{-1} for all three complexes 4–6 in the ATR-IR spectra (4 ($\tilde{\nu}$ = 2000 cm^{-1}), 5 ($\tilde{\nu}$ = 1950 cm^{-1}) and 6 ($\tilde{\nu}$ = 2013 cm^{-1})).⁴⁷ Table 1 shows these IR frequencies together with their corresponding ^{31}P NMR data.

The structure of the complex $[\text{IrPd}(\text{Cl})_3(\text{CO})(\text{P}i\text{Pr}_2\text{Im})_2]$ (**4**) in the solid state was determined by X-ray crystal structure analysis (Fig. 2).

The distance between Ir and Pd (2.6259(4) Å) is in the typical range of Ir–Pd metal bonds of similar complexes, for instance 2.614(1) Å for **6** (ref. 47) and 2.694(2) Å for $[\text{IrPd}(\text{Cl})(\text{CO})(\text{dpmp})_2]$

Table 1 ^{31}P NMR data and CO stretching frequencies for complexes 1–6

Compound	CO stretching frequencies ($\tilde{\nu}$)	^{31}P NMR chemical shift (ppm)
1	1944	28.9
2	1942	25.9
3	1971	24.4
4	2000	−0.76
5	1950	10.54
6	2013	−12.50

$[\text{PF}_6]_2$ (ref. 48) (dpmp: bis-((diphenylphosphino)methyl)-phenylphosphine). The amine functions (NH) of the two imidazolylphosphines each form a hydrogen bond to two DMSO solvent molecules in the asymmetric unit.^{52,53}

Efforts to get single crystals of the heterobimetallic complex **5** for X-ray analysis proved to be unsuccessful. DFT calculations using a well-tested hybrid-functional (TPSSH) were conducted to determine the structure of **5**, which is illustrated in Fig. 3a. The predicted Ir–Pd bond length in complex **5** (2.601 Å) is shorter than the corresponding distances in the complexes **4** and **6**.⁴⁷ In the heterobimetallic complex **5**, the highest occupied molecular orbital (HOMO) is predominantly distributed between the two metal centers, indicating significant metal–metal interaction (Fig. 3b, see SI for the corresponding molecular orbitals of **4** and **6**).

In initial catalytic studies aniline was selectively methylated using methanol, $\text{KO}t\text{Bu}$, and 0.5 mol% catalyst at 100 °C under air atmosphere, to yield *N*-methylaniline (**10a**) in 4 hours. The catalytic activities of the monometallic Ir complexes **1**, **2** and **3** were compared to those of the bimetallic catalysts **4**, **5** and **6**. The performance of bimetallic catalysts is for all cases under the

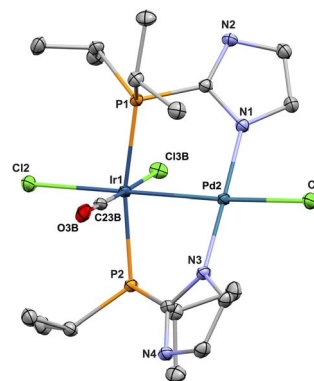


Fig. 2 Structure in the solid state of $[\text{IrPd}(\text{Cl})_3(\text{CO})(\text{P}i\text{Pr}_2\text{Im})_2]$ (**4**)·2 DMSO. DMSO molecules and hydrogen atoms have been omitted for clarity. Selected bond lengths [Å] and bond angles [°]: Ir1–Pd2 2.6259(2), Ir1–Cl2 2.5223(5), Ir1–Cl3B 2.308(5), Ir1–C23B 1.884(14), Ir1–P2 2.3473(5), Ir1–P1 2.3470(5), Pd2–Cl1 2.4098(5), Pd2–N1 2.0349(16), Pd2–N3 2.0247(16), C23B–O3B 1.20(2), P2–Ir1–P1 167.616(17), Cl2–Ir1–Pd2 178.509(14), Cl1–Pd2–Ir1 173.004(15), N3–Pd2–N1 178.00(6), C23B–Ir1–Cl3B 175.4(5). Torsion angles [°]: N1–Pd2–Ir1–P1 −36.86(5), P2–Ir1–Pd2–N3 −34.19(5).



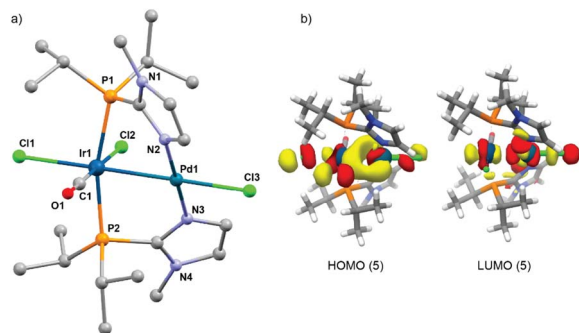


Fig. 3 (a) DFT calculated structure of $[\text{IrPd}(\text{Cl})_3(\text{CO})(\text{PiPr}_2\text{Imd}^{\text{Me}})_2]$ (**5**). (b) HOMO and LUMO for the complex **5**; DFT calculations were performed at the TPSSH/zora-def2-tzvp(-f), sarc-zora-tzvp(Ir, Pd), zora-def2-tzvp(Cl)[CPCM_{DMSO}] level of theory.

given conditions slightly better over the monometallic Iridium complexes (entries 2–7, Table 2). Kinetic profiles for the bimetallic catalysts **4**, **5** and **6** revealed that catalyst **5** gave rise to 99% yield within 3.5 hours. Catalysts **4** and **6** showed a comparable activity, reaching similar yields at a slower rate. Note that with $[\text{Ir}(\text{Cl})(\text{COD})]_2$ (ref. 70) as a catalyst, double methylation occurred (entry 1, Table 2).^{54,55}

Importantly, mixtures of the monometallic Ir (**1–3**) and Pd (**7–9**)^{56,57} catalysts (Fig. 4) showed much lower conversions under the same conditions (entries 8–10, Table 2). Replacing KOtBu with K_2CO_3 or Cs_2CO_3 as the base resulted in significantly lower conversion when using **5** as the catalytic precursor (entries 11–12, Table 2). The transformation with **5** was also

Table 2 Catalytic *N*-methylation of aniline^a

Entry	Cat.	Base	<i>T</i> (°C)	Yield ^b (%)
1 ^c	$[\text{Ir}(\text{Cl})(\text{COD})]_2$	KOtBu	100	14
2	1	KOtBu	100	83
3	2	KOtBu	100	85
4	3	KOtBu	100	83
5	4	KOtBu	100	96
6	5	KOtBu ^d	100	99
7	6	KOtBu	100	93
8	1 + 7	KOtBu	100	53
9	2 + 8	KOtBu	100	74
10	3 + <i>cis/trans</i> - 9	KOtBu	100	75
11	5	K_2CO_3	100	47
12	5	Cs_2CO_3	100	59
13	5	KOtBu	60	55
14	5	KOtBu	25	30

^a Reaction conditions: aniline (1 mmol), methanol (0.2 ml), catalyst (0.5 mol%), base (150 mol%), at 100 °C for 4 h under air atmosphere.

^b Yields were determined by GC-MS with mesitylene as the internal standard. ^c Reacting for 6 h, the selectivities towards *N*-methylaniline and *N,N*-dimethyl-aniline were 10% and 90% respectively. ^d Within 3.5 h.

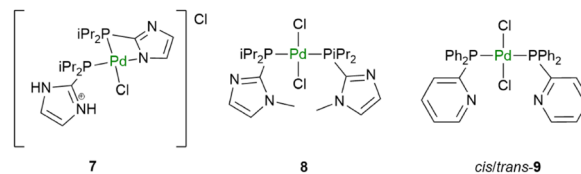
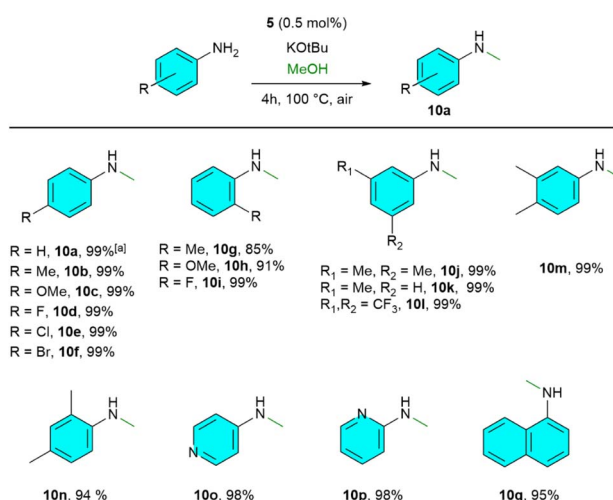


Fig. 4 Mononuclear palladium catalysts.

performed at 60 °C and room temperature (entries 13 and 14, Table 2). Although, the activities were lower showing 30% yield for the latter, homogeneous *N*-methylation at room temperature is unprecedented.^{58,59}

The scope of *N*-methylation was tested with various aniline derivatives, and catalyst **5** was efficiently able to mono-*N*-methylate diverse aromatic amines (Scheme 2). This includes *p*-substituted aromatic anilines with *p*-Me (**10b**), *p*-OMe (**10c**), and various halides (**10d–10f**), producing excellent yields (99%). The sterically hindering *o*-Me (**10g**) and *o*-OMe (**10h**) moieties slightly reduced reactivity but still produced excellent yields for *o*-F (**10i**). Additionally, 3,5-substituted anilines showed a complete conversion (**10j–10l**). Other aniline derivatives, such as 3,4-dimethyl, 2,4-dimethyl, pyridine, and naphthalene (**10m–10q**), also achieved nearly excellent yields (94–99%) of mono-*N*-methylated products.

Mechanistically it can be assumed that methanol undergoes hydrogen transfer dehydrogenation to form formaldehyde by a borrowing hydrogen mechanism mediated by the Ir center.^{60–74} The *N*-methylamine product is then obtained by hydrogenation of the *in situ* generated imine.^{70,74} To gain mechanistic insights into the *N*-methylation catalytic cycle, we examined the reactivity of complexes **4**, **5**, and **6** in independent reactions. When complex **5** was treated with MeOH under the optimized catalytic conditions, it produced the unique



Scheme 2 *N*-methylation of primary aromatic amines. Reaction conditions: amine (1 mmol), methanol (0.2 ml), base (150 mol%), **5** (0.5 mol%) at 100 °C for 4 h under air atmosphere. [a] yields for all *N*-methylated products were obtained from GC-MS analysis using mesitylene as the internal standard.



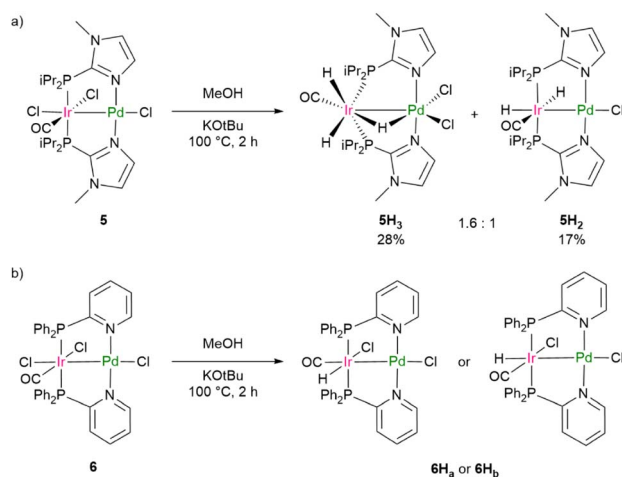
binuclear trihydrido complex **5H₃** and a dihydrido complex **5H₂** in a 1.6:1 ratio based on the ¹H NMR data (Scheme 3a). Complex **6** yielded a hydrido complex (**6H_a** or **6H_b**, Scheme 3b), which exhibits a hydrido ligand in the *cis* position to the CO ligand (Scheme 3b; (¹H NMR) $\delta = -16.58$ ppm). The reaction of complex **4** with MeOH generated a dihydrido complex in low yields, which could not be characterized further.

Independent routes to generate the complexes **5H₂** and **6H_a**/**6H_b** were also developed (Scheme 4). Complex **2** generated with MeOH and KO*t*Bu to give the mononuclear hydrido iridium complex **2H₃**, which further reacted with [Pd(Cl)₂(COD)] to yield the bimetallic complex **5H₂** (Scheme 4a). Note that a synthesis of the complex **5H₃** proved unfeasible by treatment of **5H₂** with HCl. Upon exposure of a solution of complex **3** to H₂, the dihydrido complex **3H₂** formed, as verified by X-ray crystallography (see SI). **3H₂** was then treated with [Pd(Cl)₂(COD)], producing in this case two isomeric monohydride complexes of **6H_a**/**6H_b** (Scheme 4b), one of which is the one that is also produced from **6** by reaction with MeOH.

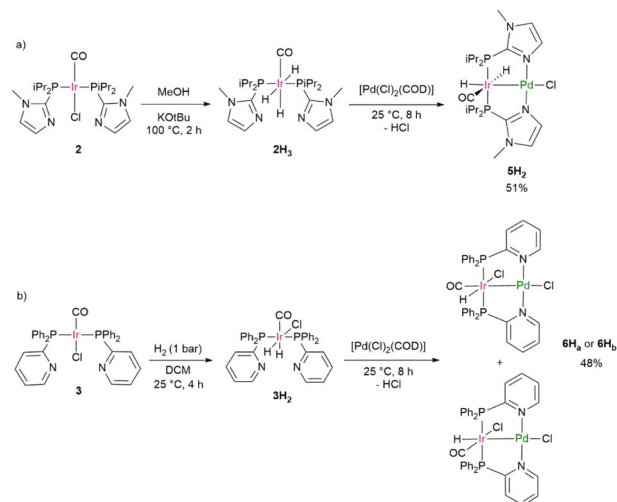
¹H NMR data for **5H₃** showed that all the hydrido ligands are located in a *cis* position to the phosphine ligands. Two signals appear as triplet of doublets and triplet of triplets signals at ($\delta = -11.97$ and -13.07 ppm, respectively) which integrate 2:1 (see SI). ²J_{H,P} coupling constants of 14.7 Hz and 19.8 Hz confirm the *cis* positions to phosphines. However, the latter hydride has a *trans* position to the CO ligand as confirmed by NMR data of the ¹³CO labeled isotopomer of **5H₃** (see SI).⁴⁷ For **5H₂** two sets of triplet of doublet signals ($\delta = -8.91$ and -20.43 ppm) with an 1:1 integration indicate the presence of two hydrido ligands (²J_{H,P} coupling constants of 18.5 Hz and 13.0 Hz, respectively).

The IR spectra of **5H₂** and **5H₃** showed three bands each: 1947, 1982, and 2097 cm⁻¹ for **5H₂**, and 2115, 1997, and 2158 cm⁻¹ for **5H₃**. These can be assigned to CO and two hydrido ligands at the iridium centers;⁴⁷ the data fit to the calculated IR spectra for **5H₂** and **5H₃** (1940/1998/2099 cm⁻¹ and 2133/2003/2169 cm⁻¹, see below).

Several attempts to obtain single crystals from the **5H₃**/**5H₂** mixture were unsuccessful due to their low stability. Therefore,



Scheme 3 Hydrido complex formation by treatment of **5** (a) and **6** (b) with MeOH.



Scheme 4 Independent synthesis of **5H₂** (a), **6H_a** and **6H_b** (b).

DFT was used to analyze the intermediates. Fig. 5 shows the optimized structures for **5H₂** and **5H₃**. Based on these structures the Ir–Pd bond lengths are 2.655 Å and 2.644 Å for **5H₃** and **5H₂** respectively. The Ir center in **5H₃** features a distorted coordination environment resulting in two hydrido ligands that could be considered magnetically equivalent as well as a bridging hydrido ligand. A comparable configuration has also been reported for binuclear Ir/Ir and Ir/Rh complexes.²⁵ Other possible isomers for **5H₃** did not converge.

The ¹H NMR spectra of the two isomers **6H_a**/**6H_b** displayed two triplet signals at $\delta = -15.39$ and -16.58 ppm (²J_{H,P} = 11.5 and 15.0 Hz respectively) in a 1:1 ratio. ¹H NMR spectra of the ¹³C isotopologues confirm the hydrides to be in the *cis* positions to the respective ¹³CO ligands (²J_{H,C} = 5.2 and 3.1 Hz, respectively).⁴⁷ The IR spectrum of a dichloromethane solution containing the isomers **6H_a** and **6H_b** revealed CO absorption bands at 2047 and 1994 cm⁻¹,⁴⁷ along with bands for the hydrido ligands at 2180 and 2192 cm⁻¹. The relative energies of the two isomers were calculated by DFT. **6H_a**, which is defined to be the complex with the hydrido ligand *trans* to Cl, is 3.15 kcal mol⁻¹ more stable than **6H_b**. Another hypothetical structure with the hydride in the *trans* position to the CO ligand **6H_c** is

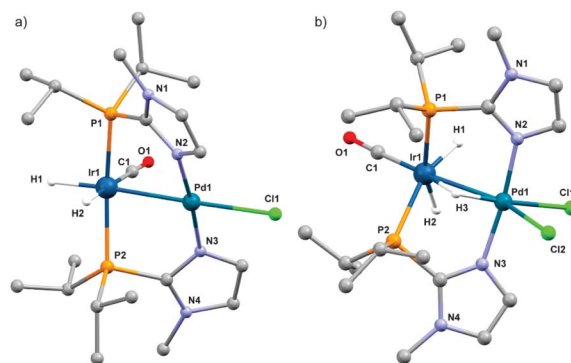


Fig. 5 DFT optimized structures of **5H₂** (a) and **5H₃** (b).



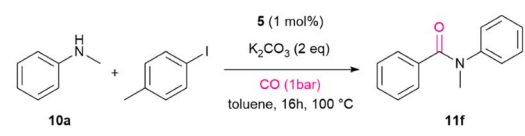
2.33 kcal mol⁻¹ less stable than **6H_a**. However, **6H_c** was ruled out by NMR spectroscopy (see above), despite thermodynamic accessibility.

Monitoring the reaction solution for the conversion of 4-fluoroaniline to give **10d** with **5** as pre-catalyst by ¹H NMR and ¹⁹F NMR spectroscopy revealed the presence of the hydrido species **5H₃** and **5H₂**, indeed (see SI). Another model reaction showed that the hydrides can act as hydrogen sources for imine hydrogenation. Thus, treatment of *N*-benzylideneaniline with a solution of **5H₃**/**5H₂** or **6H_a**/**6H_b** in the presence of methanol led to the generation of the corresponding amine with 34% and 15% yield, as confirmed by GC-MS (Scheme 5a). Note that **5H₂** is more reactive as at the end of the reaction only small amounts of **5H₃** remained. The mononuclear species **2H₃**, however, was slightly less reactive under these conditions, while **3H₂** showed no detectable conversion.^{64–69}

Notably, catalytic *N*-methylation experiments using methanol solutions of **5H₃**/**5H₂**, **6H_a**/**6H_b** produced **10a** in marginally higher yields than those reactions employing the monometallic iridium hydrides **2H₃** and **3H₂** (Scheme 5b). Experiments with methanol-d₄ and aniline resulted in the formation of labeled secondary amine. The kinetic isotope effect (KIE) for the *N*-methylation of aniline was also studied on using CH₃OH and CD₃OD. The reactions were monitored by GC-MS with mesitylene as an internal standard and a KIE value of 2.04 was determined from the ratio of initial rates (see SI).^{70,74}

Under the optimized conditions using the bimetallic catalysts for *N*-methylation (entries 5–7, Table 3), we then

Table 3 Catalytic aminocarbonylation of *N*-methylaniline^a

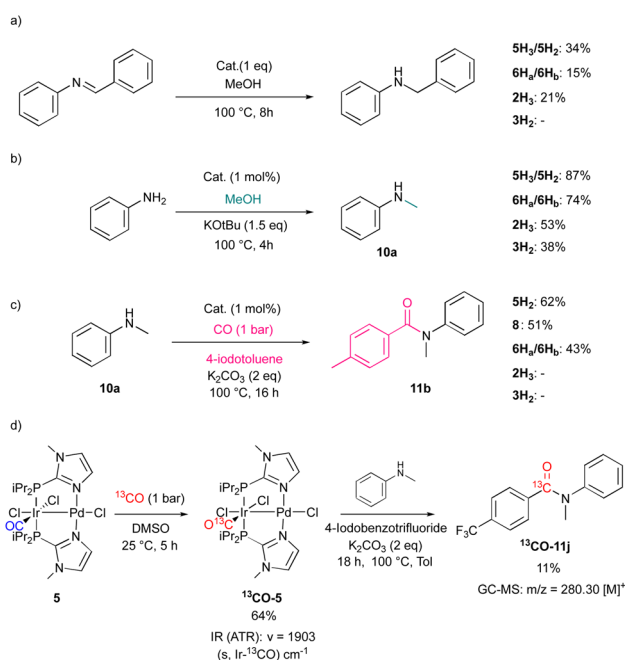


Entry	Cat.	Base	Solvent	Yield ^b (%)
1	4	K ₂ CO ₃	Toluene	80
2	5	K ₂ CO ₃	Toluene	99
3	6	K ₂ CO ₃	Toluene	77
4	7	K ₂ CO ₃	Toluene	50
5	8	K ₂ CO ₃	Toluene	51
6	9	K ₂ CO ₃	Toluene	45
7	2 + 8	K ₂ CO ₃	Toluene	30
8	3 + 9	K ₂ CO ₃	Toluene	35
9	5	K ₃ PO ₄	Toluene	70
10	5	K ₂ CO ₃	DMF	35
11	5	Et ₃ N	DMF	40

^a Reaction conditions: cat. (1 mol%), amine (1 mmol), aryl iodide (1.2 mmol), base (2 eq) and CO (1 bar). ^b Yields were determined by GC-MS with mesitylene as the internal standard.

investigated the aminocarbonylation of *N*-methylaniline. Thus, reactions of **10a** with 4-iodotoluene were run under CO atmosphere in the presence of a base using **4**, **5**, and **6** as pre-catalysts (entries 1–3, Table 3). With 1 mol% of **5** amide **11f** was formed with 85% yield when the reaction was run in the presence of K₂CO₃ as base in toluene at 100 °C within 16 h under atmospheric CO pressure (entry 1, Table 3). **5** showed a slightly better activity than **4** or **6** (entries 1 and 3, Table 3). As the carbonylation steps are presumably mainly mediated by the Pd center,^{75–94} the bimetallic systems were compared with mononuclear Pd catalysts (**7**, **8** and **9**), all showing a significant decrease in the **11f** generation (entries 4–6, Table 3). Remarkably, testing mixtures of mononuclear Ir and Pd complex corresponding to the bimetallic complexes also resulted in reduced yields (entries 7 and 8, Table 3). Moreover, using K₃PO₄ as a base with **5** as the catalyst or DMF as a solvent also gave a reduced yield (entry 9–11, Table 3). Overall, bimetallic systems outperform mononuclear counterparts in carbonylation of secondary amines, suggesting on a cooperative effect between two metal centers. Presumably, the carbonylation process is predominantly mediated by the Pd center. A classic reaction sequence involves an oxidative addition of the aryl halide, an amido complex formation, insertion of CO into the Pd–C bond, and subsequent reductive elimination of the C–N bond to yield the amide product;^{79,81,83} however, the involvement of the iridium centre in this transformation remains uncertain.

In model reactions, toluene solutions of **5H₂** and **5H₃** were then reacted with 4-iodobenzotrifluoride. The formation of trifluorotoluene as a hydrodehalogenated product with 35% yield was observed, whereas the ¹H NMR spectra showed various hydride complexes, which were not characterized further. Repeating the reaction with **6H_a**/**6H_b** did not produce trifluorotoluene.



Scheme 5 Model reactivity studies of hydrido or carbonyl complexes; (a) imine bond hydrogenation. (b) *N*-methylation of aniline using hydrido complexes. (c) Aminocarbonylation of **10a**. (d) Reactivity of **5** toward ¹³CO and its activity in the aminocarbonylation of *N*-methylaniline.

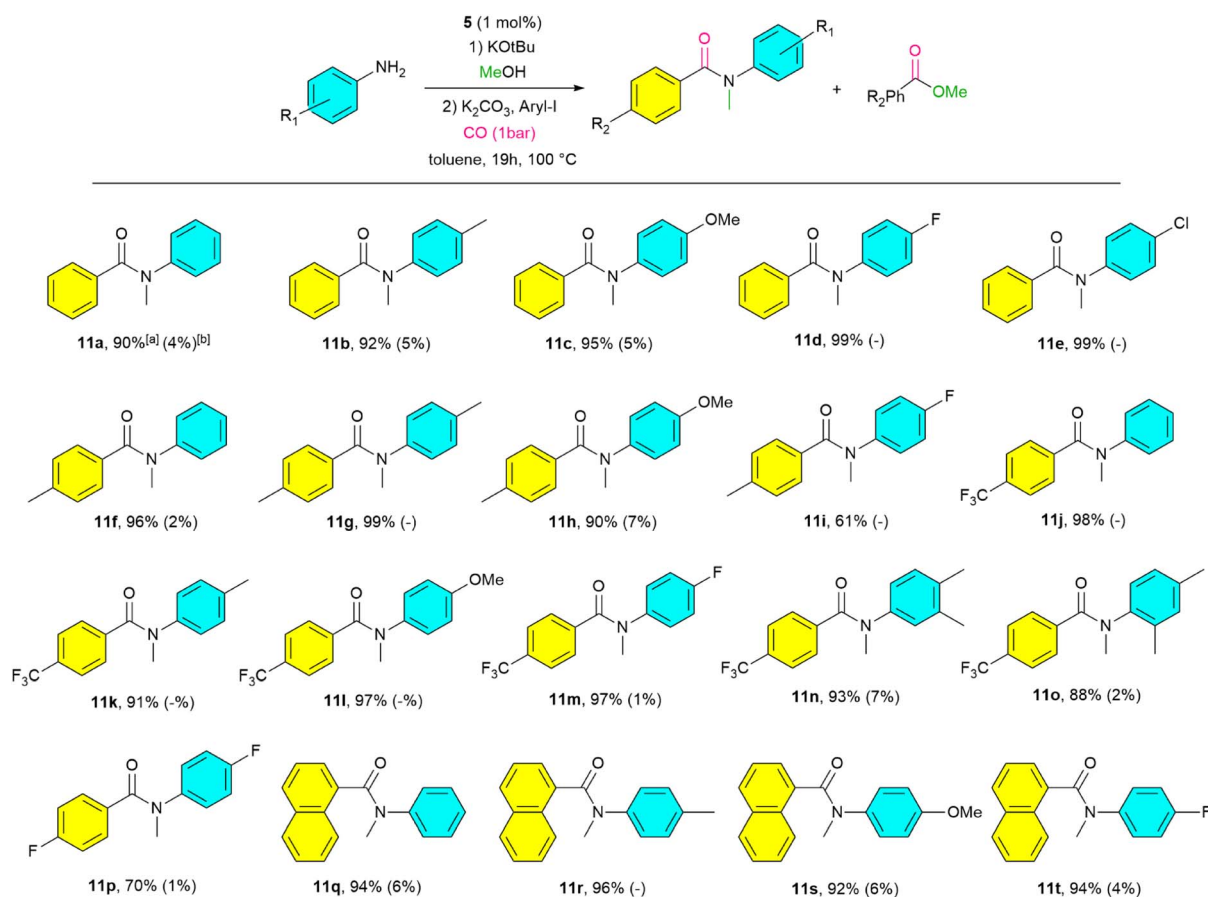


The complexes **5H₂** and **6H_a/6H_b** were then tested in the carbonylation of **10a** with 4-iodotoluene to yield successfully **11b** with 62% and 43% yield, respectively (Scheme 5c). The mononuclear Pd catalyst **8** delivered a slightly lower yield (51%) than **5H₂** (Scheme 5c). The Ir hydride species **2H₃** and **3H₂** showed no catalytic activity. Note that **5H₃** is not stable in the presence of CO, and the monohydrido complex [IrPdCl₂(H)(CO)(PiPr₂Im^{Me})₂] (**5H**) is formed under H₂ release, as confirmed by the ¹H NMR spectrum. However, after five days the generation of **5H₂** was observed (see SI). Furthermore, upon exposure of complex **5** to 1 bar atmosphere of ¹³CO, the formation of ¹³CO-**5** was observed. Note that ¹³CO-**5** could also be generated alternatively from ¹³CO-**2** carbonyl ligand exchange (see SI). *In situ*-formed ¹³CO-**5** was then treated in a stoichiometric reaction with 4-iodobenzotrifluoride and **10a** in the absence of additional CO. The generation of the ¹³C labelled carbonylation product ¹³CO-**11j** was observed (Scheme 5d). This indicates a partial participation of the Ir centre during the carbonylation step as it can provide the CO moiety for carbonylation.

The scope of the catalytic synthesis of carboxyamides was then explored on running consecutive one-pot *N*-methylation and aminocarbonylation reactions (Scheme 6). It has to be

emphasized that these conversions can also be classified as assisted-relay catalysis.⁷ Complex **5** enabled the sequential *N*-methylation of aniline derivatives with MeOH and subsequent carbonylation with iodobenzene to achieve 90–99% yields for **11a–11e**. Note that the presence of unreacted MeOH can hamper the aminocarbonylation step resulting in an esterification (Scheme 6).^{75,76}

Changing the substrate to 4-iodotoluene yielded **11f–11i**, with a reduced yield for **11i**. Using 4-iodobenzotrifluoride increased yields for **11j–11m** with fully converted aniline and 4-fluoroaniline to **11j**, **11l** and **11m**, with decreased esterification and maintaining good yields for **11n–11o**. Note that **11l–11o** were not described before. In contrast, 4-fluoroaniline and 4-fluoroiodobenzene gave significantly lower yields (**11p**). The use of 1-iodonaphthalene⁷⁷ as the aryl halide afforded high yields (**11q–11t**), with excellent selectivity for naphthamides formation. We also exploited bromobenzene and chlorobenzene as aryl halide substrates. With aniline as substrate only traces of **11a** were produced. However, 1-bromonaphthalene yielded 55% of **11p**. Note that, in contrast, two literature reported examples for nitroarene methylation and a subsequent carbonylation using a palladium acetate/phosphine system under higher CO pressure proceeded *via* a two-step process.⁹⁵



Scheme 6 Catalyzed *N*-methylation and subsequent carbonylation using various aryl iodides. Reaction conditions: amine (1 mmol), MeOH (0.2 ml), KOtBu (1.5 eq), K₂CO₃ (2 eq), aryl iodide (1.2 eq), **5** (1 mol%), toluene (3 ml). ^aAll yields are isolated yields. ^bYields for esterification are shown in the parentheses.



Conclusions

In conclusion, we developed a unique one-pot process for the selective mono-*N*-methylation of primary amines that is coupled with an aminocarbonylation. Bimetallic iridium/palladium complexes were used as catalytic precursors. The approach introduces both alkyl and carbonyl functionalities in two coupled catalytic cycles, offering advantages concerning atom economy and synthetic efficiency. Remarkably, the bimetallic catalysts outperform their monometallic counterparts in both *N*-methylation and carbonylation. The former is presumably mainly mediated by the iridium center, whereas for the latter the palladium center seems to be crucial. In model reactions hydrido complexes could be identified as possible intermediates. In addition, the developed method requires only 1 bar of CO and there is no need for high-pressure setups.^{81,93}

Author contributions

Conceptualization, A. A., T. B. and M. R.; experimental and theoretical studies, A. A., K. K. and P. W.; X-ray crystallography, O. H.; writing – original draft preparation, A. A.; writing – review and editing, A. A., P. W. and T. B.; funding acquisition, T. B.

Conflicts of interest

There are no conflicts to declare.

Data availability

CCDC 2430139 (2), 2430140 (3H₂) and 2430141 (4) contain the supplementary crystallographic data for this paper.^{96a-c}

Supplementary information: details of the experimental procedures, characterization of the complexes and the DFT calculated details. See DOI: <https://doi.org/10.1039/d5sc03892h>.

Acknowledgements

This work was funded by the Deutsche Forschungsgemeinschaft (DFG, German Research Foundation) under Germany's Excellence Strategy – EXC 2008 – 390540038 – UniSysCat.

Notes and references

- N. T. Patil, V. S. Shinde and B. Gajula, *Org. Biomol. Chem.*, 2012, **10**, 211.
- A. Ajamian and J. L. Gleason, *Angew. Chem., Int. Ed.*, 2004, **43**, 3754.
- J. C. WasilkeS, J. Obrey, R. T. Baker and G. C. Bazan, *Chem. Rev.*, 2005, **105**, 1001.
- D. E. Fogg and E. N. Dos Santos, *Coord. Chem. Rev.*, 2004, **248**, 2365.
- J. M. Lee, Y. Na, H. Han and S. Chang, *Chem. Soc. Rev.*, 2004, **33**, 302.
- F. Rudroff, M. D. Mihovilovic, H. Gröger, R. Snajdrova, H. Iding and U. T. Bornscheuer, *Nat. Catal.*, 2018, **1**, 12.
- S. Martínez, L. Veth, B. Lainer and P. Dydio, *ACS Catal.*, 2021, **11**, 3891.
- D. R. Pye and N. P. Mankad, *Chem. Sci.*, 2017, **8**, 1705.
- A. Grossmann and D. Enders, *Angew. Chem., Int. Ed.*, 2012, **51**, 314.
- P. Buchwalter, J. Rosé and P. Braunstein, *Chem. Rev.*, 2015, **115**, 28.
- R. Maity, B. S. Birenheide, F. Breher and B. Sarkar, *ChemCatChem*, 2021, **13**, 2337.
- M. H. Pérez-Temprano, J. A. Casares and P. Espinet, *Chem.–Eur. J.*, 2012, **18**, 1864.
- M. Shibasaki, H. Sasai and T. Arai, *Angew. Chem., Int. Ed.*, 1997, **36**, 1236.
- M. M. Lorion, K. Maindan, A. R. Kapdi and L. Ackermann, *Chem. Soc. Rev.*, 2017, **46**, 7399.
- J. Campos, *Nat. Rev. Chem.*, 2020, **4**, 696.
- D. C. Powers and T. Ritter, *Nat. Chem.*, 2009, **1**, 302.
- P. Braunstein and A. A. Danopoulos, *Chem. Rev.*, 2021, **121**, 7346.
- S. Sabater, J. A. Mata and E. Peris, *Nat. Commun.*, 2013, **4**, 2553.
- J. P. Stambuli, R. Kuwano and J. F. Hartwig, *Angew. Chem., Int. Ed.*, 2002, **41**, 4746.
- E. K. van den Beuken and B. L. Feringa, *Tetrahedron*, 1998, **54**, 12985.
- A. Majumder, R. Naskar, P. Roy, B. Mondal, S. Garai and R. Maity, *Dalton Trans.*, 2023, **52**, 2272.
- A. Majumder, T. Nath Saha, N. Majumder, R. Naskar, K. Pal and R. Maity, *Eur. J. Inorg. Chem.*, 2021, 1104.
- K. Kretschmar, V. Pelmenchikov, M. Kaupp, T. Braun, P. Wittwer, S. Rachor and J. Cardozo, *Eur. J. Inorg. Chem.*, 2023, **26**, e202300099.
- A. Majumder, R. Naskar, P. Roy and R. Maity, *Eur. J. Inorg. Chem.*, 2019, **13**, 1810.
- T. Nakajima, M. Kotani, Y. Maeda, M. Sato, K. Iwai and T. Tanase, *Inorg. Chem.*, 2024, **63**, 19847.
- Y. Zhang, S. P. Roberts, R. G. Bergman and D. H. Ess, *ACS Catal.*, 2015, **5**, 1840.
- S. Huang, X. Hong, H. Z. Cui, B. Zhan, Z. M. Li and X. F. Hou, *Organometallics*, 2020, **39**, 3514.
- K. M. Gramigna, D. A. Dickie, B. M. Foxman and C. M. Thomas, *ACS Catal.*, 2019, **9**, 3153.
- S. Patra and N. Maity, *Coord. Chem. Rev.*, 2021, **434**, 213803.
- M. A. Esteruelas, M. P. Garcia, A. M. Lopez and L. A. Oro, *Organometallics*, 1991, **10**, 127.
- J. T. Moore and C. C. Lu, *J. Am. Chem. Soc.*, 2020, **142**, 11641.
- C. Fricke, T. Sperger, M. Mendel and F. Schoenebeck, *Angew. Chem., Int. Ed.*, 2021, **60**, 3355.
- J. A. Mata, F. E. Hahn and E. Peris, *Chem. Sci.*, 2014, **5**, 1723.
- S. Gonell, M. Poyatos, J. A. Mata and E. Peris, *Organometallics*, 2012, **31**, 5606.
- J. Fu, X. Huo, B. Li and W. Zhang, *Org. Biomol. Chem.*, 2017, **15**, 9747.
- Z. Mandegani, A. Nahaei, M. Nikraves, S. M. Nabavizadeh, H. R. Shahsavari and M. M. Abu-Omar, *Organometallics*, 2020, **39**, 3879.



- 37 L. G. Pezuk, B. Sen, F. E. Hahn and H. Turkmen, *Organometallics*, 2019, **38**, 593.
- 38 R. C. Nishad, S. Kumar and A. Rit, *Organometallics*, 2021, **40**, 915.
- 39 N. Hazari, P. R. Melvin and M. M. Beromi, *Nat. Rev. Chem.*, 2017, **1**, 0025.
- 40 K. J. Bonney, F. Proutiere and F. Schoenebeck, *Chem. Sci.*, 2013, **4**, 4434.
- 41 D. P. Hruszkewycz, D. Balcells, L. M. Guard, N. Hazari and M. Tilset, *J. Am. Chem. Soc.*, 2014, **136**, 7300.
- 42 M. Aufiero, T. Scattolin, F. Proutiere and F. Schoenebeck, *Organometallics*, 2015, **34**, 5191.
- 43 G. Magnin, J. Clifton and F. Schoenebeck, *Angew. Chem., Int. Ed.*, 2019, **58**, 10179.
- 44 E. E. Martinez, M. R. Moreno, C. A. Barksdale and D. J. Michaelis, *Organometallics*, 2021, **40**, 2763.
- 45 A. Zanardi, J. A. Mata and E. Peris, *Chem.–Eur. J.*, 2010, **16**, 10502.
- 46 A. Zanardi, J. A. Mata and E. Peris, *J. Am. Chem. Soc.*, 2009, **131**, 14531.
- 47 G. Franciò, R. Scopelliti, C. G. Arena, G. Bruno, D. Drommi and F. Faraone, *Organometallics*, 1998, **17**, 338.
- 48 A. L. Balch and V. J. Catalano, *Inorg. Chem.*, 1992, **31**, 2569.
- 49 J. P. Farr, M. M. Olmstead and A. L. Balch, *J. Am. Chem. Soc.*, 1980, **102**, 6654.
- 50 T. W. Mak, *J. Chem. Soc. Dalton Trans.*, 1997, **19**, 3409.
- 51 S. M. Kuang, F. Xue, T. C. Mak and Z. Z. Zhang, *Inorg. Chim. Acta*, 1999, **284**, 119.
- 52 T. Steiner, *Angew. Chem., Int. Ed.*, 2002, **41**, 48.
- 53 S. Sander, R. Muller, M. Ahrens, M. Kaupp and T. Braun, *Chem.–Eur. J.*, 2021, **27**, 14287.
- 54 G. Cho and S. H. Hong, *Angew. Chem., Int. Ed.*, 2018, **57**, 6166.
- 55 S. Zhang, J. J. Ibrahim and Y. Yang, *Org. Chem. Front.*, 2019, **6**, 2726.
- 56 J. J. de Pater, C. E. P. Maljaars, E. de Wolf, M. Lutz, A. L. Spek, B. J. Deelman, C. J. Elsevier and G. van Koten, *Organometallics*, 2005, **24**, 5299.
- 57 J. Liu, C. Jacob, K. J. Sheridan, F. Al-Mosule, B. T. Heaton, J. A. Iggo, M. Matthews, J. Pelletier, R. Whyman, J. F. Bickley and A. Steiner, *Dalton Trans.*, 2010, **39**, 7921.
- 58 M. Nielsen, E. Alberico, W. Baumann, H. J. Drexler, H. Junge, S. Gladiali and M. Beller, *Nature*, 2013, **495**, 85.
- 59 V. N. Tsarev, Y. Morioka, J. Caner, Q. Wang, R. Ushimaru, A. Kudo, H. Naka and S. Saito, *Org. Lett.*, 2015, **17**, 2530.
- 60 A. Corma, J. Navas and M. J. Sabater, *Chem. Rev.*, 2018, **118**, 1410.
- 61 S. Bähn, S. Imm, L. Neubert, M. Zhang, H. Neumann and M. Beller, *ChemCatChem*, 2011, **3**, 1853.
- 62 T. D. Nixon, M. K. Whittlesey and J. M. Williams, *Dalton Trans.*, 2009, **5**, 753.
- 63 M. H. S. Hamid, P. A. Slatford and J. M. Williams, *Adv. Synth. Catal.*, 2007, **349**, 1555.
- 64 S. Çakır, S. B. Kavukcu, O. Sahin, S. Gunnaz and H. Turkmen, *ACS Omega*, 2023, **8**, 5332.
- 65 T. T. Dang, B. Ramalingam and A. M. Seayad, *ACS Catal.*, 2015, **5**, 4082.
- 66 E. Podyacheva, O. I Afanasyev, D. V. Vasilyev and D. Chusov, *ACS Catal.*, 2022, **12**, 7142.
- 67 S. N. R. Donthireddy, P. Mathoor Illam and A. Rit, *Inorg. Chem.*, 2020, **59**, 1835.
- 68 X. Ye, P. N. Plessow, M. K. Brinks, M. Schelwies, T. Schaub, F. Rominger, R. Paciello, M. Limbach and P. Hofmann, *J. Am. Chem. Soc.*, 2014, **136**, 5923.
- 69 S. Elangovan, J. Neumann, J. B. Sortais, K. Junge, C. Darcel and M. Beller, *Nat. Commun.*, 2016, **7**, 12641.
- 70 M. González-Lainez, M. V. Jiménez, R. Azpiroz, V. Passarelli, F. J. Modrego and J. J. Pérez-Torrente, *Organometallics*, 2022, **41**, 1364.
- 71 C. Gunanathan and D. Milstein, *Science*, 2013, **341**, 1229712.
- 72 G. E. Dobreiner and R. H. Crabtree, *Chem. Rev.*, 2010, **110**, 681.
- 73 J. Templ and M. Schnürch, *Chem.–Eur. J.*, 2024, **30**, e202304205.
- 74 J. Ji, Y. Huo, Z. Dai, Z. Chen and T. Tu, *Angew. Chem., Int. Ed.*, 2024, **63**, e202318763.
- 75 T. Xu and H. Alper, *J. Am. Chem. Soc.*, 2014, **136**, 16970.
- 76 L. Kollár, A. Takács, C. Molnár, A. Kovács, L. T. Mika and P. Pongrácz, *J. Org. Chem.*, 2023, **88**, 5172.
- 77 W. Fang, Q. Deng, M. Xu and T. Tu, *Org. Lett.*, 2013, **15**, 3678.
- 78 L. Ran, Z. H. Ren, Y. Y. Wang and Z. H. Guan, *Chem.–Asian J.*, 2014, **9**, 577.
- 79 A. Schoenberg and R. F. Heck, *J. Org. Chem.*, 1974, **39**, 3327.
- 80 C. L. Allen and J. M. J. Williams, *Chem. Soc. Rev.*, 2011, **40**, 3405.
- 81 A. Brennführer, H. Neumann and M. Beller, *Angew. Chem., Int. Ed.*, 2009, **48**, 4114.
- 82 J. Y. Wang, A. E. Strom and J. F. Hartwig, *J. Am. Chem. Soc.*, 2018, **140**, 7979.
- 83 J. R. Martinelli, T. P. Clark, D. A. Watson, R. H. Munday and S. L. Buchwald, *Angew. Chem., Int. Ed.*, 2007, **46**, 8460.
- 84 F. C. Rix, M. Brookhart and P. S. White, *J. Am. Chem. Soc.*, 1996, **118**, 4746.
- 85 P. Hermange, A. T. Lindhardt, R. H. Taaning, K. Bjerglund, D. Lupp and T. Skrydstrup, *J. Am. Chem. Soc.*, 2011, **133**, 6061.
- 86 B. Aranda, S. A. Moya, A. Vega, G. Valdebenito, S. Ramirez-Lopez and P. Aguirre, *Appl. Organomet. Chem.*, 2019, **33**, e4709.
- 87 P. J. Tambade, Y. P. Patil and B. M. Bhanage, *Appl. Organomet. Chem.*, 2009, **23**, 235.
- 88 S. D. Friis, T. Skrydstrup and S. L. Buchwald, *Org. Lett.*, 2014, **16**, 4296.
- 89 C. F. J. Barnard, *Organometallics*, 2008, **27**, 5402.
- 90 L. Kollár, *Modern Carbonylation Methods*, Wiley-VCH Verlag, Weinheim, Germany, 2008.
- 91 J. R. Martinelli, D. A. Watson, D. M. Freckmann, T. E. Barder and S. L. Buchwald, *J. Org. Chem.*, 2008, **73**, 7102.
- 92 H. Du, Q. Ruan, M. Qi and W. Han, *J. Org. Chem.*, 2015, **80**, 7816.
- 93 S. T. Gadge and B. M. Bhanage, *RSC Adv.*, 2014, **4**, 10367.
- 94 A. Mohanty, S. Sadhukhan, M. K. Nayak and S. Roy, *J. Org. Chem.*, 2024, **89**, 1010.
- 95 L. Wang, H. Neumann and M. Beller, *Angew. Chem., Int. Ed.*, 2019, **58**, 5417.



- 96 (a) A. Abdolrahimi, P. Woite, K. Kretschmar, M. Roemelt, T. Braun and O. He, CCDC 2430139: Experimental Crystal Structure Determination, 2025, DOI: [10.5517/ccdc.csd.cc2mkrmlk](https://doi.org/10.5517/ccdc.csd.cc2mkrmlk); (b) A. Abdolrahimi, P. Woite, K. Kretschmar, M. Roemelt, T. Braun and O. He, CCDC 2430140: Experimental Crystal Structure Determination, 2025, DOI: [10.5517/ccdc.csd.cc2mkrml](https://doi.org/10.5517/ccdc.csd.cc2mkrml); (c) A. Abdolrahimi, P. Woite, K. Kretschmar, M. Roemelt, T. Braun and O. He, CCDC 2430141: Experimental Crystal Structure Determination, 2025, DOI: [10.5517/ccdc.csd.cc2mkrnm](https://doi.org/10.5517/ccdc.csd.cc2mkrnm).

